Isolating and Localizing ATP-Sensitive Tryptophan Emission in Skeletal Myosin Subfragment 1†

Sungjo Park and Thomas P. Burghardt*

Department of Biochemistry and Molecular Biology, Mayo Foundation, 200 First Street Southwest, Rochester, Minnesota 55905

Received April 25, 2000; Revised Manuscript Received July 12, 2000

ABSTRACT: The fluorescence intensity difference between rabbit skeletal myosin subfragment 1 (S1) and nucleotide-bound or trapped S1 isolates ATP-sensitive tryptophans (ASTs) emission from the total tryptophan signal. Neutral (acrylamide) quenching of the ASTs is sensitive to the binding or trapping of nucleotide to the active site of S1. Anion (I^-) quenching of the ASTs, sensitive to charge separation in the tryptophan micro environment, is negligible. These findings suggest the ASTs sense conformational change during ATPase from negatively charged surroundings. Specific chemical modifications of S1 identified the location of the ASTs. Trp131 was quenched by chemical modification, and its emission was isolated by taking the intensity difference between unmodified and modified S1. Trp131 fluorescence intensity and quenching constant do not distinguish among the bound or trapped nucleotides, suggesting that the vicinity of Trp131 does not change conformation during the ATPase cycle and eliminating Trp131 as an AST. Trp510 fluorescence was quenched by 5′-iodoacetamidofluorescein (5′IAF) modification of the reactive thiol (SH1) of S1. The tryptophan emission enhancement increment due to active site trapping decreases linearly with SH1 modification and extrapolates to 0 for 100% modification. These data identify Trp510 as the primary AST in skeletal S1 in agreement with observations from Dictyostelium (Batra and Manstein (1999) *Biol. Chem. 380*, 1017−1023) and smooth muscle S1 (Yengo et al. (2000) *Biophys. J. 78*, 242A). With Trp510 identified as the sole AST, fluorescence difference spectroscopy provides a novel means to monitor the concentration of myosin transient intermediates in ATP hydrolysis.

Tryptophan fluorescence enhancement upon ATP binding to myosin subfragment 1 (S1) is a well-known indicator of conformational change. Chymotryptic skeletal myosin S1 contains five tryptophan (Trp) residues positioned at 113, 131, 440, 510, and 595. Trp113 and 131 are in the 27-kDa subunit, and the other three tryptophans are in the 50-kDa subunit. Fluorescence lifetimes (*2*), acrylamide quenching of tryptic fragments (*3*, *4*), spatial proximity mapping (*5*), and chemical modification (*6*−*9*) of S1 have been used to identify the ATP-sensitive tryptophans (ASTs) with inconsistent results. By isolating signals from single tryptophan residues with site-directed mutagenesis, Trp510 was shown to be the primary AST in Dictyostelium S1 (DcS1) (*10*) and smooth muscle (*11*).

Like others, we sought to identify the residues responsible for tryptophan fluorescence enhancement upon ATP binding in skeletal myosin. We isolated the Trp510 fluorescence signal with specific chemical modification and fluorescence difference spectroscopy. Trp510 changes intensity and solvent accessibility, indicating conformational changes in its vicinity during ATP hydrolysis (*12*, *13*). However, we did not rule out the possibility that other tryptophan residues also contributed to the total fluorescence increase upon ATP binding.

In the present study, we are again concerned with the identity of the ASTs and their sensitivity to local myosin conformation. We isolated the Trp131 fluorescence signal with specific chemical modification and fluorescence difference spectroscopy, and measured its enhancement and acrylamide quenching in the absence and presence of nucleotide or trapped nucleotide analogues. By a similar difference technique that does not require any chemical modification of the system, we isolated the ASTs' fluorescence in S1 and measured their enhancement and accessibility to acrylamide and KI quenchers. Our data show that Trp510 is the residue in S1 responsible for ATP sensitivity and that it detects conformational changes in the probe binding cleft during the ATPase cycle in agreement with our earlier work (*12*, *13*). Preliminary data to this study have been reported previously (*14*).

THEORY

Differential Spectroscopy. We isolate selected tryptophans in S1 using differential spectroscopy. The difference of fluorescence intensities, ΔI, between S1 and perturbed S1,

† This work was supported by the National Institutes of Health Grant R01 AR39288 and the Mayo Foundation.

* Telephone: 507-284-8120. Fax: 507-284-9349. E-mail: burghardt@mayo.edu.

[1] Abbreviations: AlF_4^-, aluminum fluoride complex; AST, ATP-sensitive tryptophan; BeF_x, beryllium fluoride complex; Cys707 or SH1, most reactive thiol in myosin subfragment 1; DcS1, dictyostelium myosin subfragment 1; DHNBS, dimethyl(2-hydroxy-5-nitrobenzyl)-sulfonium bromide; 5′IAF(IAA)-S1, 5′-iodoacetamidofluorescein (iodoacetamide)-labeled S1; DHNBS−S1, DHNBS-modified myosin subfragment 1; S1, myosin subfragment 1; Trp 131 (510), tryptophan 131(510) in chicken pectoralis muscle myosin sequence (Note: myosin sequence numbering throughout the manuscript is that of chicken pectoralis muscle (*1*). When denoting S1 in the presence of nucleotide or when trapped with nucleotide analogue the presence of Mg is implicit and not usually stated.)

10.1021/bi000945t CCC: $19.00
Published on Web 08/31/2000

$$\Delta I = I(\mathrm{S1}, -) - I(\mathrm{S1}, \mathrm{P}) \quad (1)$$

isolates tryptophan fluorescence from the perturbed residues. A perturbation is structural (the binding of substrate to the active site) or chemical (modification of a tryptophan or cysteine residue). Considering the sources of the emitted fluorescence from eq 1,

$$\Delta I(\mathrm{S1}, -, \mathrm{f}, \mathrm{P}, \mathrm{f}') \propto \sum_i \{\phi_i(-,\mathrm{f}) - \phi_i(\mathrm{P}, \mathrm{f}')\} \quad (2)$$

where the sum is over the tryptophans perturbed by P, and ϕ_i is the quantum efficiency for the ith residue. The argument for the macroscopic quantity ΔI includes a global parameter (the system S1) and several other parameters pertaining to isolated tryptophans that fully specify the experimental system. Pairs of the isolated tryptophan parameters are ordered in ΔI such that $\Delta I(\mathrm{S1}, -, \mathrm{f}, \mathrm{P}, \mathrm{f}') = -\Delta I(\mathrm{S1}, \mathrm{P}, \mathrm{f}', -, \mathrm{f})$. Single-tryptophan-defined quantities such as the quantum efficiency, lifetime, or Stern−Volmer quenching constant, have two arguments stating the perturbant followed by the S1 conformer. Different but unspecified conformers are represented by f, f′, f″, ... The perturbants we use are as follows: −(no perturbant), 5′IAF, DHNBS, ATP, ADP, and, ADP·PA (the ADP phosphate analogues). The S1 conformers are as follows: −(S1 alone), *(M*·ATP), **(M**·ADP·Pi), ^(M^·ADP), and ◇(denoting the heterogeneous conformation of S1 in the presence of ATP).

Perturbers and conformers are independent for a chemical perturbant because the chemically perturbed S1 can bind any nucleotide or analogue to induce a conformer but a nucleotide or nucleotide analogue perturbant can have only one conformer. When the quantum efficiency (or any single-tryptophan-defined quantity) has a nucleotide or nucleotide analogue perturbant then the following rule applies: (i) the quantity is equal to the same unperturbed quantity in the appropriate conformation. For instance, the ADP perturbed quantum efficiency, ϕ(ADP, ^), equals $\phi(-, ^)$, the unperturbed value in the ^ conformation. The ATP perturber is a special case because S1 has several conformers in steady-state ATPase but formally Rule (i) still holds because we defined ◇ to denote a heterogeneous conformation.

Quantum efficiency in terms of excited-state relaxation rates is

$$\phi_i = \frac{k_{\mathrm{F},i}}{\Gamma_i + k_{\mathrm{q},i}[\mathrm{Q}]} \quad (3)$$

where k_F is the intrinsic fluorescence relaxation rate, k_q is the relaxation rate due to interaction with Q, and Γ is the sum of all rates leading to excited-state decay excluding k_q. We expect each of these rates to change with perturbation of S1. The fluorescence lifetime in the absence of quencher is $\tau_i = (\Gamma_i)^{-1}$ giving with eqs 2 and 3,

$$\Delta I(\mathrm{S1}, -, \mathrm{f}, \mathrm{P}, \mathrm{f}') \propto \sum_i \left\{ \frac{k_{\mathrm{F},i}(-, \mathrm{f})\tau_i(-, \mathrm{f})}{1 + k_{\mathrm{q},i}(-, \mathrm{f})\tau_i(-, \mathrm{f})[\mathrm{Q}]} - \frac{k_{\mathrm{F},i}(\mathrm{P}, \mathrm{f}')\tau_i(\mathrm{P}, \mathrm{f}')}{1 + k_{\mathrm{q},i}(\mathrm{P}, \mathrm{f}')\tau_i(\mathrm{P}, \mathrm{f}')[\mathrm{Q}]} \right\} \quad (4)$$

Noting that $K_{\mathrm{sv},i} = k_{\mathrm{q},i}\tau_i$ is the Stern−Volmer constant and $\phi_{0,i} = k_{\mathrm{F},i}\tau_i$ is the quantum efficiency in the absence of quencher,

$$\Delta I(\mathrm{S1}, -, \mathrm{f}, \mathrm{P}, \mathrm{f}') \propto \sum_i \left\{ \frac{\phi_{0,i}(-, \mathrm{f})}{1 + K_{\mathrm{SV},i}(-, \mathrm{f})[\mathrm{Q}]} - \frac{\phi_{0,i}(\mathrm{P}, \mathrm{f}')}{1 + K_{\mathrm{SV},i}(\mathrm{P}, \mathrm{f}')[\mathrm{Q}]} \right\} \quad (5)$$

We relate quantum efficiencies between two conformations of S1 in the absence of quencher with eq 5 such that

$$\frac{\Delta I(\mathrm{S1}, -, -, \mathrm{P}, \mathrm{f})}{\Delta I(\mathrm{S1}, -, -, \mathrm{P}', \mathrm{f}')} = \frac{\sum_i \{\phi_{0,i}(-, -) - \phi_{0,i}(\mathrm{P}, \mathrm{f})\}}{\sum_i \{\phi_{0,i}(-, -) - \phi_{0,i}(\mathrm{P}', \mathrm{f}')\}} \quad (6)$$

where P and P′ would specify different perturbants if they are nucleotides.

The ratio of the difference of intensities in the absence and presence of quencher from eq 5, $\Delta I_0/\Delta I$, gives

$$\frac{\Delta I_0}{\Delta I}(\mathrm{S1}, -, \mathrm{f}, \mathrm{P}, \mathrm{f}') = \frac{\sum_i \{\phi_{0,i}(-, \mathrm{f}) - \phi_{0,i}(\mathrm{P}, \mathrm{f}')\}}{\sum_i \left\{ \frac{\phi_{0,i}(-, \mathrm{f})}{1 + K_{\mathrm{SV},i}(-, \mathrm{f})[\mathrm{Q}]} - \frac{\phi_{0,i}(\mathrm{P}, \mathrm{f}')}{1 + K_{\mathrm{SV},i}(\mathrm{P}, \mathrm{f}')[\mathrm{Q}]} \right\}} \quad (7)$$

Expanding the right-hand side of eq 7 in a Taylor series about [Q] = 0,

$$\frac{\Delta I_0}{\Delta I}(\mathrm{S1}, -, \mathrm{f}, \mathrm{P}, \mathrm{f}') \approx 1 + [\mathrm{Q}] \left\{ \frac{\sum_i \phi_{0,i}(\mathrm{P}, \mathrm{f}')K_{\mathrm{SV},i}(\mathrm{P}, \mathrm{f}') - \phi_{0,i}(-, \mathrm{f})K_{\mathrm{SV},i}(-, \mathrm{f})}{\sum_i \phi_{0,i}(\mathrm{P}, \mathrm{f}') - \phi_{0,i}(-, \mathrm{f})} \right\} \quad (8)$$

to first order in [Q]. We define the coefficient of [Q] in eq 8 to be the effective quenching constant, K_eff. K_eff is a weighted difference of Stern−Volmer constants for unperturbed and perturbed tryptophan species, i.e., a macroscopic observable quantity defined by tryptophans in two different conformations. Its argument list is defined identically to that of ΔI. Although it is tempting to use K_eff to judge tryptophan accessibility to solvent, this is not generally permissible, and only the Stern−Volmer constant should be used in that context. We use eqs 6 and 8 exclusively for nucleotide or nucleotide analogue perturbants and designate this by replacing P with N. For a single AST and using Rule (i), eq 6 and K_eff become

$$\frac{\phi_{0,1}(\mathrm{N}, \mathrm{f})}{\phi_{0,1}(-, -)} = 1 - \frac{\Delta I(\mathrm{S1}, -, -, \mathrm{N}, \mathrm{f})}{\Delta I(\mathrm{S1}, -, -, \mathrm{N}', \mathrm{f}')} \left\{ 1 - \frac{\phi_{0,1}(-, \mathrm{f}')}{\phi_{0,1}(-, -)} \right\} \quad (9)$$

$$K_{SV,1}(N, f) = \left\{1 - \frac{\phi_{0,1}(-, f')}{\phi_{0,1}(-, f)}\right\} K_{eff}(S1, -, f', N, f) + \frac{\phi_{0,1}(-, f')}{\phi_{0,1}(-, f)} K_{SV,1}(-, f') \quad (10)$$

Equations 9 and 10 are recursive, relating one single tryptophan quantity with another without defining absolute value. Absolute quantities $\phi_{0,1}(-, f')/\phi_{0,1}(-, f)$ and $K_{SV,1}(-, f')$, provided by the chemical perturbant experiments discussed next, prime the recursive formulas for the computation of the quantum efficiency ratio and Stern−Volmer constants from experiments with perturbant N. The perturbed single tryptophan quantities appearing on the left-hand sides of eqs 9 and 10 are likewise observable from chemical perturbant experiments using S1's with bound nucleotides providing the means to compare the two methods, understanding that they are not fully independent. Finally, the choice of f′ (from which N′ follows) is arbitrary in eq 9 such that experimental accuracy and convenience could determine its choice.

The Special Case of Chemical Perturbants. When P is a chemical perturbation that eliminates fluorescence from a specific tryptophan residue, as in the modification of Trp131 with DHNBS or the quenching of Trp510 by modification of SH1 (*6*, *15*, *16*), $\phi_{0,i}$(DHNBS or 5′IAF, f) = 0. We perform experiments with the intensity difference taken between two samples of the same conformer (one sample chemically perturbed, the other chemically unperturbed). The ratio of observations from two conformations gives, from eq 2,

$$\frac{\Delta I(S1, -, f, C, f)}{\Delta I(S1, -, f', C, f')} = \frac{\phi_{0,1}(-, f)}{\phi_{0,1}(-, f')} \quad (11)$$

where we have substituted C for P to denote that the perturbation is chemical. This is the ratio needed in eqs 9 and 10. Under similar conditions, quenching experiments from conformation f, give exactly from eq 5,

$$\frac{\Delta I_0}{\Delta I}(S1, -, f, C, f) = 1 + [Q] K_{SV,1}(-, f) \quad (12)$$

i.e., the Stern−Volmer equation for unperturbed S1 in conformation f, a quantity needed in eq 10. Evidentially, the quantum efficiency and Stern−Volmer constants in eqs 11 and 12 are significant in their own right as they tell about the nucleotide-induced quantum efficiency and quencher accessibility changes in a particular residue of S1.

Samples used in experiments with chemically perturbed S1 contain varying fractions of modified and unmodified protein due to the imperfect efficiency of normal specific chemical modification techniques. The intensity from such a sample, $a_1 I(S1, C, f) + (1 - a_1) I(S1, -, f)$ where a_1 is the fractional concentration of the chemically perturbed S1, subtracted from the intensity of the unperturbed sample, $a_1 I(S1, -, f) + (1 - a_1) I(S1, -, f)$, gives the real intensity difference $\Delta I_R(S1, -, f, C, f) = a_1\{I(S1, C, f) - I(S1, -, f)\} = a_1 \Delta I(S1, -, f, C, f)$. Constant a_1 cancels when forming the intensity ratios in eqs 11 and 12, removing any dependence on the fractional concentration.

In another application, we utilize a difference signals dependence on a_1. Consider the intensity difference ΔI(5′IAF−S1, N, f, −, −) = I(5′IAF−S1, N, f) − I(5′IAF−S1, −, −). Note that the global system parameter is the probe-modified protein (5′IAF−S1) rather than the usual S1, and that the perturbation is a nucleotide or nucleotide analogue, N. Recall that modification of S1 with 5′IAF totally eliminates Trp510 fluorescence. The real intensity difference, $\Delta I_R(a_1[5'IAF-S1] + \{1 - a_1\}[S1], N, f, -, -) = a_1\{I(5'IAF-S1, N, f) - I(5'IAF-S1, -, -)\} + \{1 - a_1\}\{I(S1, N, f) - I(S1, -, -)\}$. Forming a ratio from ΔI_R and the intensity for a sample with global parameter S1 and perturbation N,

$$\Delta i_R(N) \equiv \frac{\Delta I_R(a_1[5'IAF-S1] + \{1 - a_1\}[S1], N, f, -, -)}{\Delta I(S1, N, f, -, -)} = a_1 \frac{\Delta I(5'IAF - S1, N, f, -, -)}{\Delta I(S1, N, f, -, -)} + 1 - a_1 \quad (13)$$

The observable on the left-hand side, $\Delta i_R(N)$, is the normalized tryptophan enhancement increment due to nucleotide binding to a sample containing $a_1 \times$ [5′IAF−S1] plus $\{1 - a_1\} \times$ [S1]. This is equal to $a_1 \times$ {the normalized enhancement increment from ASTs other than Trp510} plus $\{1 - a_1\} \times$ {the normalized enhancement increment from all ASTs including Trp510}. The value of $\Delta i_R(N)$ when $a_1 = 1$, i.e., the normalized enhancement increment from ASTs other than Trp510, determines whether tryptophans other than Trp510 contribute to AST emission.

Conventional Quenching of S1. By considerations identical to those used to derive eqs 5 and 8, the dynamic quenching of S1 containing several inequivalent tryptophans has

$$\frac{I_0}{I}(S1) \approx 1 + [Q] \frac{\sum_i K_{SV,i} \phi_{0,i}}{\sum_i \phi_{0,i}} \quad (14)$$

to first order in [Q]. The sum in i is over the inequivalent tryptophan species. When there is one tryptophan, eq 14 is exactly the Stern−Volmer equation.

Distribution of Transient States during ATPase. Myosin-catalyzed ATP hydrolysis consists of the elementary steps shown in Scheme 1.

Scheme 1

$$M + ATP \rightleftarrows M^*\cdot ATP \rightleftarrows M^{**}\cdot ADP\cdot Pi \rightleftarrows M^{\wedge}\cdot ADP + Pi \rightleftarrows M + ADP + Pi$$

In this scheme, M, M*, M**, and M^ represent distinct transient conformational states of myosin (*17*). Shorthand for the heterogeneous conformer of myosin in the presence of ATP is $M^{\diamond}$. Nonhydrolyzable nucleotides or nucleotide analogues bound to, or trapped in, S1 induce static conformations associated with these transient intermediates. Crystallographic and solution structural data suggest that the static structures induced by trapped ADP−AlF_4^- or ADP−BeF_x mimic the M**·ADP·Pi or M*·ATP intermediates, and bound ADP mimics M^·ADP (*17*−*21*).

The distribution of the transient intermediates in Scheme 1 varies with temperature and other experimental conditions. Bagshaw and Trentham (*17*) showed that at 21 °C and 0.1 M KCl, 5 mM $MgCl_2$, and 50 mM Tris-HCl, pH 8, S1 + ATP in the steady-state consists of 87% M**·ADP·Pi, 9%

M*·ATP, and 4% M^·ADP. They also showed that in the same conditions, but at 5 °C, S1 + ATP in the steady-state consists of 55−64% M**·ADP·Pi, 5−6% M*·ATP, and 30−40% M^·ADP. These data are useful to us for two reasons. First, S1 + ATP at the higher temperature condition is essentially the M**·ADP·Pi conformer. As such, we obtain intensity and quenching data directly from the transient intermediate. Second, the known distribution of transient intermediates for S1 + ATP can be compared with our observations by the method discussed next.

During steady-state ATPase, the total fluorescence intensity from S1 is a sum of intensities from each transient species in Scheme 1 weighted by their fractional concentrations, c_i. The fractional concentration of the M state is negligible in the presence of the ∼0.2 mM nucleotide used in our experiments (*17*), consequently, for for a single AST,

$$\phi_{0,1}(-, {}^{\diamond}) = c_1\phi_{0,1}(-, *) + c_2\phi_{0,1}(-, **) + c_3\phi_{0,1}(-, {}^{\wedge}) \quad (15)$$

and

$$c_1 + c_2 + c_3 = 1 \quad (16)$$

By a slight generalization of eq 12, we obtain an expression relating Stern−Volmer constants for S1 in steady-state ATPase with those from the transient intermediates,

$$K_{SV,1}(-, {}^{\diamond}) = [c_1\phi_{0,1}(-, *)K_{SV,1}(-, *) + c_2\phi_{0,1}(-, **)K_{SV,1}(-, **) + c_3\phi_{0,1}(-, {}^{\wedge})K_{SV,1}(-, {}^{\wedge})]/[c_1\phi_{0,1}(-, *) + c_2\phi_{0,1}(-, **) + c_3\phi_{0,1}(-, {}^{\wedge})] \quad (17)$$

Equations 15−17 are a system of equations constraining the c_i's when the Stern−Volmer constants and quantum efficiency ratios, parameters measurable from chemical perturbation experiments, are known. With the additional inequality constraints $0 \le c_i \le 1$, we may solve for the least squares values of the c_i's.

Substitution of eqs 9 and 10 into eqs 15 and 17 provides the equivalent relationships for the effective quenching constants and intensity differences directly observable with the nucleotide perturbation experiments. We find

$$\Delta I(\mathrm{ATP}, {}^{\diamond}) = c_1\Delta I(N_1, *) + c_2\Delta I(N_2, **) + c_3\Delta I(N_3, {}^{\wedge}) \quad (18)$$

$$K_{eff}(\mathrm{ATP}, {}^{\diamond}) = [c_1\Delta I(N_1, *)K_{eff}(N_1, *) + c_2\Delta I(N_2, **)K_{eff}(N_2, **) + c_3\Delta I(N_3, {}^{\wedge})K_{eff}(N_3, {}^{\wedge})]/[c_1\Delta I(N_1, *) + c_2\Delta I(N_2, **) + c_3\Delta I(N_3, {}^{\wedge})] \quad (19)$$

where N_1, N_2, and N_3 are nucleotide or analogue perturbants that induce the M*, M**, and M^ conformations, respectively, and all arguments are preceded with (S1, −, −, ...).

When applying eqs 15 and 17−19, we use the nucleotide analogues ADP−BeF_x, ADP−AlF_4^-, and ADP to induce the M*, M**, and M^ conformations, respectively.

MATERIALS AND METHODS

Chemicals. Dimethyl(2-hydroxy-5-nitrobenzyl)sulfonium bromide (DHNBS), 5′-iodoacetamidofluorescein (5′IAF), iodoacetamide (IAA), ADP, ATP, α-chymotrypsin, dithiothreitol (DTT), phenylmethanesulfonyl fluoride (PMSF), ethylenediaminetetraacetic acid (EDTA), potassium chloride (KCl), potassium iodide (KI), potassium thiosulfate ($K_2S_2O_3$), aluminum chloride ($AlCl_3$), and magnesium chloride ($MgCl_2$) were from Sigma (St. Louis, MO). Potassium fluoride (KF) was from Fluka (Switzerland). Acrylamide (ultrapure) was from ICN (Aurora, OH). All other chemicals were reagent grade.

Solutions. KI stock solution (3 M) was prepared with a small amount of $K_2S_2O_3$ (∼0.1 mM) to prevent I_3^- formation. The KI solution was stored in the dark and used within a few days of preparation. Acrylamide stock solution (3 M) was also stored in the dark. A stock solution of $BeCl_2$ (88 mM Be, atomic absorption standard solution in 1% HCl) was adjusted to pH 5.0 by addition of NaOH. A stock solution of KF (1 M) was prepared fresh each day in a plastic bottle.

Preparation and Labeling of Myosin S1. Rabbit myosin was prepared by a standard method (*22*), and S1 was prepared by digesting myosin filaments with α-chymotrypsin (*23*). DHNBS modification of Trp131 in S1 (DHNBS−S1) was carried out as described previously (*6*, *24*). Unreacted DHNBS was removed by exhaustive dialysis (four times) against 20 mM Tris-HCl, 1 mM EDTA, and 150 mM KCl or NaCl, pH 7.8, and gel filtration on a Sephadex PD10 column (Pharmarcia, Uppsala, Sweden) with 25 mM TES, pH 7. DHNBS concentration in DHNBS−S1 was determined in the presence of 0.14 N NaOH (pH > 12) by absorption at 410 nm using $\epsilon_{410} = 18\,400\ M^{-1}\ cm^{-1}$. Protein concentration in DHNBS−S1 was measured by Bradford BioRad microassay or by absorption corrected for the contribution of DHNBS at 280 nm where $\epsilon_{280} = 2500\ M^{-1}\ cm^{-1}$. We incorporated 0.85−1.25 DHNBS groups per S1. The K^+−EDTA and Ca^{2+} ATPase of DHNBS−S1 were 96 ± 8% and 138 ± 20%, respectively, of the native S1.

5′IAF modification of SH1 in S1 (5′IAF−S1) was carried out with 0.5−1.5-fold molar excess of 5′IAF for 18−20 h at 4 °C in the dark as described previously (*25*). We incorporated 0.25−0.71 5′IAF groups per S1 as determined by K^+−EDTA and Ca^{2+} ATPase activities (*26*, *27*). Unreacted 5′IAF was normally not removed from the 5′IAF−S1 samples because we found that its presence did not influence the tryptophan fluorescence observed in our experiments.

IAA modification of SH1 in S1 (IAA−S1) was carried out in conditions identical to those for 5′IAF except that 1.5−25-fold molar excess of IAA was used. The incorporated IAA groups per S1 were 0.20−0.65 as determined by K^+−EDTA and Ca^{2+} ATPase activities.

Myosin S1 ATPase. ATPase activity of S1 was measured from organic phosphate production using the Fiske and Subbarow method (*28*) and expressed as percent of control S1. K^+−EDTA ATPase measurements were made on samples at 25 °C from 1 mL aliquots containing 0.26−0.35 μM S1, 2 mM ATP, 0.6 M KCl, 25 mM Tris-HCl, pH 8, and 6 mM EDTA. Ca^{2+} ATPase was measured as for K^+−EDTA ATPase except that 6 mM $CaCl_2$ replaced the 6 mM EDTA.

Preparation of Nucleotide-Bound or Trapped Nucleotide Analogue S1, DHNBS−S1, and 5′IAF−S1. Myosin S1 or 5′IAF−S1 was trapped as described previously (*28*). DHNBS−S1 (10−20 μM) in 25 mM TES, pH 7.0, was mixed with 1 mM $MgCl_2$, 0.2 mM ADP, 10 mM KF, and 0.2 mM

$AlCl_3$ (or $BeCl_2$) and then incubated for 20 min at 25 °C. When trapped, K^+−EDTA activities for S1 and DHNBS−S1, and Ca^{2+} ATPase activities for 5′IAF−S1 were inhibited by ≥90%. For experiments in the presence of nucleotide, S1, DHNBS−S1, or 5′IAF−S1 was incubated with 1 mM $MgCl_2$ and 0.25 mM ATP or ADP.

Spectroscopic Measurements. We measured fluorescence on a SLM 8000 spectrofluorometer (SLM instruments, Urbana, IL) with monochromator slits of 1−2 nm. Tryptophans in 1−1.5 μM S1, DHNBS−S1, or 5′IAF−S1 were excited with 295−300 nm light, and we estimated tryptophan emission intensity using the area from the emission band integrated from 315 to 360 nm.

Fluorescence Quenching. Acrylamide and KI quenching experiments were conducted at 6 and 20 °C in 25 mM TES, pH 7. For KI quenching, constant ionic strength conditions were maintained by addition of KCl such that [KCl] + [KI] = 0.4 M.

We investigated the nature of the acrylamide and KI quenching mechanisms of tryptophans in S1 by observing quenching curves for each system at two temperatures (6 and 20 °C). Acrylamide quenching efficiency increased with increasing temperature, indicating the predominance of dynamic or collisional quenching over the static quenching mechanism. In contrast, KI quenching efficiency decreased with increasing temperature, indicating the predominance of the static over the dynamic quenching mechanism.

All quenching data were plotted as a function of quencher concentration using eqs 8, 12, or 14. These data were fitted with the line $y = 1 + Kx$ by linear least squares for free parameter K. The correlation between x and y measures the model's appropriateness such that a value of <1 indicates nonlinear contributions to the data from noise and/or systematic sources.

RESULTS

Fluorescence Enhancement and Acrylamide Quenching of Trp131. DHNBS specifically modifies the indole ring of Trp131, and the modified indole does not fluoresce, giving $\phi_{0,Trp131}(DHNBS, f) = 0$ (*6*). The chemically modified S1 (DHNBS−S1) shows minimal perturbation of essential determinants of protein function such as the actin-activated, Ca^{2+}, and K^+−EDTA ATPase suggesting that the native structure of the S1 remains intact except for the modified side chain. Under these circumstances, the difference of intensities in eq 1 with DHNBS as the perturbant can reasonably be assumed to isolate Trp131 emission such that eqs 11 and 12 apply.

The fluorescence enhancement and acrylamide quenching Stern−Volmer constants of Trpl31 were measured using eqs 11 and 12, and the results are summarized in Table 1. We found that substrate binding caused fluorescence enhancements of 16−25% with ATP causing the largest increase. The fluorescence enhancements, while significantly different from 1, were not dependent on the type of bound substrate. Like the fluorescence enhancements, the Trp131 Stern−Volmer constant changes upon substrate binding, but the constants are not dependent on the type of bound substrate. This behavior is very different from that observed for Trp510 (see Table 2). The insensitivity of these parameters to the various substrates involved in, or mimicking those in, the ATPase cycle suggests that Trpl31 is not a significant contributor to the AST emission.

Table 1: Trp131 Fluorescence Enhancements and Stern−Volmer Acrylamide Quenching Constants at 20 °C[a]

nucleotide or analogue	S1 conform. (f)	$\frac{\phi_{0,Trp131}(-, f)}{\phi_{0,Trp131}(-, -)}$	$K_{SV,Trp131}(-, f)$
		1	10.21 ± 0.53 (4)
ADP−BeF_x	M*	1.19 ± 0.01 (2)	9.27 ± 0.08 (2)
ADP−AlF_4^-	M**	1.16 ± 0.05 (3)	8.93 ± 0.34 (3)
ADP	M^	1.19 ± 0.03 (3)	9.38 ± 0.03 (3)
ATP	M◇	1.25 ± 0.02 (3)	8.54 ± 0.27 (4)

[a] Constants measured using eqs 11 and 12 with chemical perturbant C = DHNBS. S1 conformations are from Scheme 1. Quenching constants are in units of M^{-1}. Errors are standard error of the mean with (n) observations.

Table 2: Trp510 Fluorescence Enhancements and Stern−Volmer Acrylamide Quenching Constants at 20 °C[a]

nucleotide or analogue	S1 conform. (f)	$\frac{\phi_{0,Trp510}(-, f)}{\phi_{0,Trp510}(-, -)}$	$K_{SV,Trp510}(-, f)$	[c][b]
		1	9.91 ± 0.36(3)	0
ADP−BeF_x	M*	1.58 ± 0.02(2)	7.57 ± 0.18(2)	0.02
ADP−AlF_4^-	M**	2.02 ± 0.02(2)	5.67 ± 0.02(2)	0.88
ADP	M^	1.38 ± 0.05(3)	9.72 ± 0.13(3)	0.10
ATP	M◇	1.95 ± 0.06(3)	6.20 ± 0.16(3)	
ATP (computed)[c]	M◇	2.0	6.2	

[a] Constants measured using eqs 11 and 12 with chemical perturbant C = 5′IAF. S1 conformations are from Scheme 1. Quenching constants are in units of M^{-1}. Errors are standard error of the mean with (n) observations. [b] Fractional concentration in steady-state ATPase computed by simultaneously solving eqs 15−17. [c] From eqs 15 and 17 using the data in the table.

Isolation of ASTs Other than Trp510. Trp510 is a known AST (*9*−*12*, *29*). The possibility that the ASTs include residues other than Trp510 was considered using 5′IAF to specifically modify SH1 in S1. There, the probe completely quenches Trp510 fluorescence giving $\phi_{0,Trp510}(5'IAF, f) = 0$, but it is too distant from other tryptophans in S1 to affect their fluorescence (*15*, *16*). Modification of SH1, in and of itself, does not alter tryptophan emission in S1 without nucleotide or when S1 assumes other conformational states induced by nonhydrolyzable nucleotide or nucleotide analogues (*30*). Under these circumstances, the difference of intensities in eq 1 with 5′IAF as the perturbant can reasonably be assumed to isolate Trp510 emission such that eqs 11−13 apply.

Figure 1 shows the normalized tryptophan emission enhancement increment due to active site trapping by ADP−AlF_4^-, Δi_R(ADP−AlF_4^-), as a function of the extent of 5′IAF modification of SH1. This increment, proportional to the normalized enhancement increment from ASTs other than Trp510 as shown in eq 13, decreases linearly with SH1 modification. The linear extrapolation to 100% modification indicates there is no significant AST emission when Trp510 is quenched. We conclude that Trp510 is the sole AST.

For comparison, we replaced 5′IAF at SH1 with IAA and performed identical measurements. The IAA at SH1 cannot quench Trp510 but indicates the effect of the modification of SH1 on the observed intensity ratio. Data in Figure 1 shows that modification of SH1 with IAA has no significant effect on the intensity ratio, as expected from eq 13 if S1 and IAA−S1 are spectroscopically identical. These results with 5′IAF and IAA substantiate that the predominant contribution to AST emission comes from Trp510.

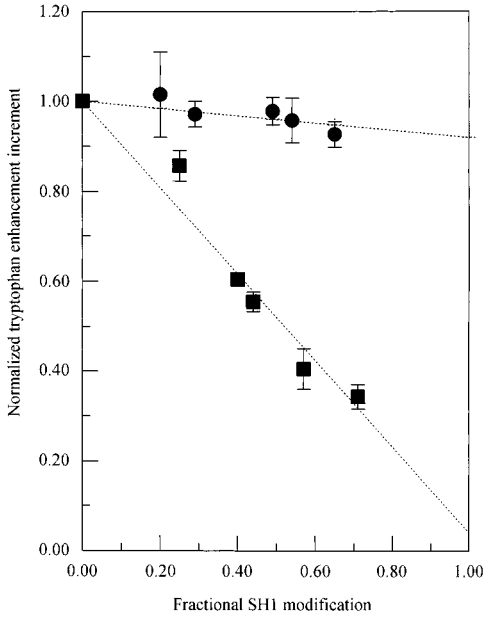

FIGURE 1: Normalized tryptophan enhancement increment due to ADP−AlF_4^- trapping of the active site of S1, Δi_R(ADP−AlF_4^-) (■), as a function of the fractional SH1 modification by 5′IAF. Equation 13 defines Δi_R. For comparison, IAA (●) was substituted for 5′IAF and identical measurements performed. The data were fitted with lines constrained to start at 1 using a least-squares protocol. The correlation values for the fitted lines are 0.982 for modification with 5′IAF or 0.842 for modification with IAA. Error bars indicate standard error of the mean. All observations were made in 25 mM TES, pH 7, at 20 °C.

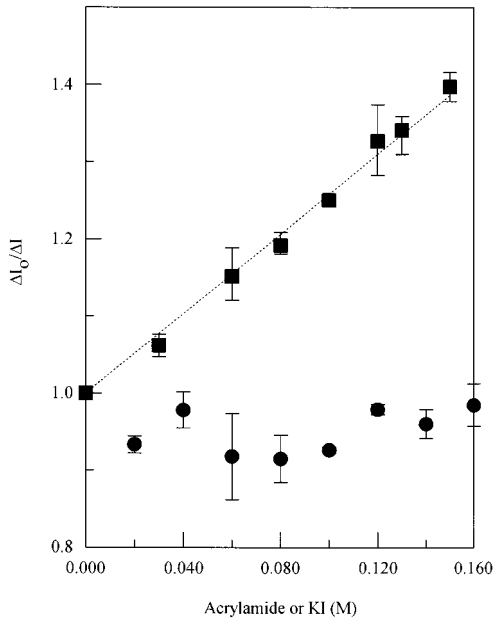

FIGURE 2: Acrylamide (■) or KI (●) quenching of AST emission at high ionic strength with ATP as the structural perturbant. The effective acrylamide quenching constant, defined in eq 8, was computed from the slope of the curve to be 2.64 ± 0.16 M^{-1} (error estimate from $n = 3$ observations). The correlation value for the fitted line is 0.995. Error bars indicate standard error of the mean. Observations were made in 25 mM TES, pH 7, at 6 °C. Ionic strength conditions were identical in the samples due to addition of 0.4 M KCl to the acrylamide-quenched sample or by maintaining [KCl] + [KI] = 0.4 M for the KI quenched sample.

Fluorescence Enhancement and Acrylamide Quenching of Trp510. The fluorescence enhancements and Stern−Volmer constants of Trp510 due to nucleotide binding were measured using eqs 11 and 12 with 5′IAF as the chemical perturbant. The results are summarized in Table 2. We find that changes in the fluorescence enhancements and, the Stern−Volmer constants indicating Trp510 exposure to solvent, follow the progression of the S1 conformation through the steps in the ATPase cycle, as reported previously (*12*). We showed previously that the structural changes in S1 accompanying ATP hydrolysis correlate with the size of the substrate, illustrating an aspect of the mechanism of energy transduction in myosin (*13*).

We now can also estimate the occupancy of the steady-state ATPase transients from S1 + ATP because Trp510 is the sole AST. Equations 15−17 relate fluorescence enhancements and Stern−Volmer constants of Trp510 with the fractional concentrations, c_i, of the steady-state ATPase intermediates in Scheme 1. These three equations, plus the constraints $0 \leq c_i \leq 1$, produce a linear least-squares solution for the c_i's. Table 2 shows the fractional concentrations for 20 °C. We find that the M**·ADP·Pi state is the predominant intermediate as expected for this temperature (*17*).

Fluorescence Enhancement and Quenching of the ASTs. Data described above (in *Isolation of ASTs Other than Trp510*) identify Trp510 as the principal AST, implying interchangeability of AST and Trp510. Some results discussed below are interpreted under the assumption that the AST residues are just Trp510 while others are more general in nature and are independent of the number and identity of ASTs. Subsequently, we refer to ASTs when we wish to imply the more general conclusion.

We isolated AST emission using eq 1 with bound ATP as the structural perturbant and observed the KI and acrylamide quenching of this system at 6 °C. Figure 2 shows the $\Delta I_0/\Delta I$ versus [Q] plots, with slope indicating the effective quenching constants according to eq 8, for the KI and acrylamide quenching. KI is an anionic quencher that senses the microenvironment of tryptophan because of charge interactions (*31*). The effective KI quenching constant is very nearly zero, indicating that I^- could not readily access the ASTs. The KI quenching experiments require unusually high ionic strength conditions where [KCl] + [KI] = 400 mM. For comparison, we observed the acrylamide quenching of the ASTs at low, moderate, and high ionic strength where [KCl] = 0, 60, and 400 mM, respectively. The effective acrylamide quenching constant of the ASTs decreases with increasing ionic strength but remains significant even when [KCl] = 400 mM (shown in Figure 2), indicating that the inaccessibility of KI to the ASTs is not likely due to high ionic strength. Notwithstanding the just summarized results, the data in Figure 2 show that for $[I^-] \geq 0.02$ M, I^- enters into a weak but detectable concentration independent interaction with Trp510 causing (by inspection of eq 7) a slight enhancement of fluorescence from this residue in the M conformation, a slight decrease in this emission efficiency in the $M^{\diamond}$ conformation, or both.

We isolated AST emission using eq 1 with bound nucleotide or trapped nucleotide analogue as the structural perturbant and observed the fluorescence enhancement and acrylamide quenching at 20 °C. The AST fluorescence quantum efficiency enhancements were computed using eq 9, primed with data from Table 2 for Trp510 and the ADP conformation of S1. The results are summarized in Table 3.

Table 3: AST (Trp510) Effective Fluorescence Enhancement and Acrylamide Quenching Constants at 20 °C[a]

nucleotide or analogue (N)	S1 conformation (f)	$\frac{\Delta I(S1, -, -, N, f)}{\Delta I(S1, -, -, ADP, ^)}$	$K_{eff}(S1, -, -, N, f)$	[c][b]	$\frac{\phi_{0,Trp510}(N, f)}{\phi_{0,Trp510}(-, -)}$	$K_{SV,Trp510}(N,f)$
ADP−BeF_x	M*	1.61 ± 0.03(2)	4.45 ± 0.07 (2)	0.22	1.6	7.8
ADP−AlF_4^-	M**	2.62 ± 0.08(2)	3.17 ± 0.21 (2)	0.74	2.0	6.5
ADP	M^	1	5.01 ± 0.03 (3)	0.04	1.4	8.6
ATP	M◇	2.38 ± 0.07(4)	3.51 ± 0.10 (4)	−	1.9	6.8
ATP (computed)[c]	M◇	2.4	3.5	−	−	−

[a] Effective fluorescence enhancements and acrylamide quenching constants, $\frac{\Delta I(S1, -, -, N, f)}{\Delta I(S1, -, -, ADP, ^)}$ and $K_{eff}(S1, -, -, N, f)$, are from eqs 6 and 8, respectively, with perturbant P = N and P′ = ADP. Fluorescence enhancements and Stern−Volmer quenching constants, $\frac{\phi_{0,Trp510}(N, f)}{\phi_{0,Trp510}(-, -)}$ and $K_{SV,Trp510}(N, f)$ are from eqs 9 and 10, respectively, primed with data taken from Table 2. The S1 conformations are from Scheme 1. Quenching constants are in units of M^{-1}. Errors are standard error of the mean with (*n*) observations. [b] Fractional concentration in steady-state ATPase computed by simultaneously solving eqs 16, 18, and 19. [c] From eqs 18 and 19 using the data in the table.

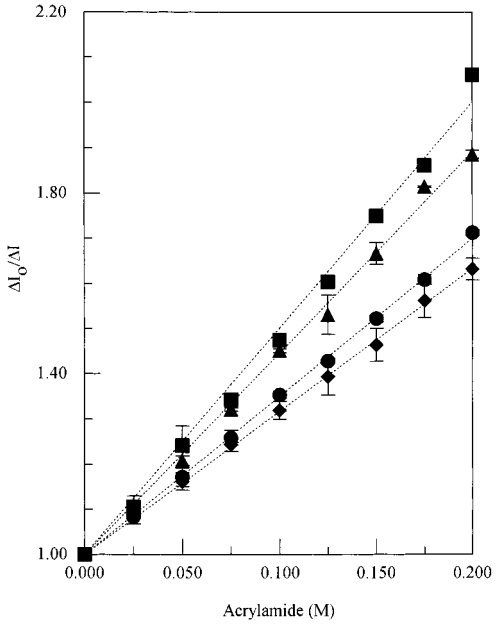

FIGURE 3: Acrylamide quenching of AST emission with ADP (■), $ADPBeF_x$ (▲), ATP (●), and $ADPAlF_4^-$ (◆) as the structural perturbants. The effective acrylamide quenching constants, defined in eq 8, were computed from the slopes of the curves and listed in Table 3. The correlation values for the fitted lines are 0.999 (0.998 for ADP). Error bars indicate standard error of the mean. All observations were made in 25 mM TES, pH 7, at 20 °C.

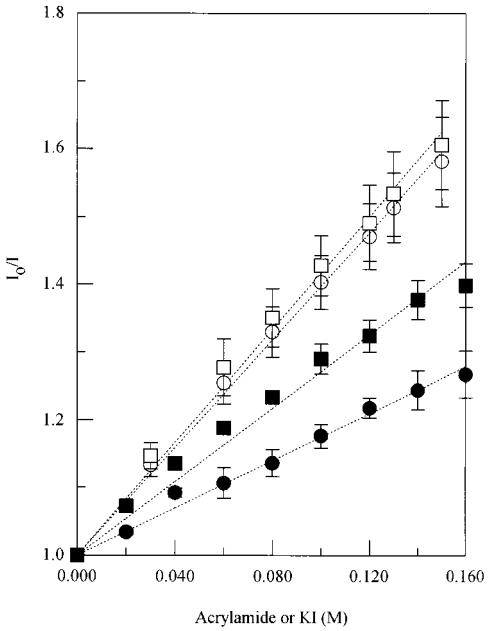

FIGURE 4: Acrylamide or KI quenching of total tryptophan fluorescence from S1. Acrylamide (unfilled) or KI (filled) quenched S1 in the absence (■ or □) and presence (● or ○) of ATP. The average Stern−Volmer quenching constants, defined in eq 14, in the absence and presence of ATP are 3.79 ± 0.31 (*4*) and 3.68 ± 0.23 M^{-1} (*4*), respectively. The average KI quenching constants in the absence and presence of ATP are 2.61 ± 0.15 (3) and 1.68 ± 0.13 M^{-1} (3), respectively. Error estimates are from *n* observations in conditions identical to that indicated in the caption to Figure 2. The fitted line correlation values for acrylamide (KI) quenching are 0.998 (0.994) and 0.999 (0.997) for S1 and S1 + ATP, respectively.

The fluorescence enhancements so computed compare favorably with the equivalent quantities in Table 2.

Figure 3 shows the $\Delta I_0/\Delta I$ versus [Q] plots, with slope indicating the effective quenching constants according to eq 8, for the AST acrylamide quenching. The Stern−Volmer constants were computed using eq 10, primed with data from Table 2 for Trp510 and the ADP conformation of S1. The results are summarized in Table 3. The Stern−Volmer constants so computed compare favorably with the equivalent quantities in Table 2. We find that Trp510 is least accessible to acrylamide when ADP−AlF_4^- traps the active site of S1 and most accessible when ADP is bound to the active site. The quenching constant of the ASTs in the presence of ATP is closest to that for trapped $ADPAlF_4^-$.

We estimate the occupancy of the steady-state ATPase transients from S1 + ATP using the fluorescence enhancements and effective quenching constants from Table 3 with eqs 16, 18, and 19, and the constraints $0 \le c_i \le 1$. Table 3 shows the fractional concentrations for 20 °C. We find that the M**·ADP−Pi state is again the predominant intermediate as expected for this temperature (*17*) and in rather good agreement with the results from Table 2.

Recalling that the distribution of transient S1 conformations in ATPase at 20 °C heavily favors the M** intermediate (see Scheme 1), we identify the effective and Stern−Volmer quenching constants for S1 + ATP with those of M**. The observation that at 20 °C the quenching constants of the ASTs in the presence of ATP is closest to that for trapped $ADPAlF_4^-$ further justifies the identification.

Total Tryptophan Fluorescence Quenching. We observed the acrylamide or KI quenching of S1 total tryptophan fluorescence in the absence and presence of ATP at 6 °C. Figure 4 shows the plots of I_0/I versus [Q] that, from eq 14, give the average Stern−Volmer constants. The average

Stern−Volmer constants for acrylamide quenching in the absence and presence of ATP, 3.79 and 3.68 M^{-1} respectively, indicate no significant change in average tryptophan accessibility to a neutral quencher, in agreement with earlier results (*9*). The average Stern−Volmer constants for KI quenching in the absence and presence of ATP are 2.61 ± 0.15 (*3*) and 1.68 ± 0.13 (*3*) M^{-1}, respectively. Quenching with KI shows a significant difference between S1 and S1 + ATP such that iodide has less average accessibility to tryptophan residues in S1 + ATP. The finding with KI is consistent with results observed from heavy meromyosin (*32*, *33*).

S1 total tryptophan fluorescence is the summed emission from five residues. The observed Stern−Volmer constant for this system, given by eq 14, is a weighted average of Stern−Volmer constants for each residue with weights equal to the fractional emitted intensities. We observed the average acrylamide Stern−Volmer constant to be insensitive to ATP binding to S1. Evidently acrylamide quenching acquires significant ATP sensitivity only when the ASTs are selectively observed as in Figures 2 and 3.

The result in Figure 4 with KI suggests that ATP directly inhibits KI quenching of one or more tryptophans that are not ATP-sensitive. Possibly, local charge separation on the ATP molecule when bound to the active site repels KI from the vicinity of a tryptophan residue without sterically hindering access to this residue by neutral acrylamide. Trp131 is not involved in this scenario since its KI quenching does not sense ATP binding (data not shown). Other candidates are Trp113 and Trp440.

DISCUSSION

Isolating and Specifying the AST. It is widely known that many kinds of S1 increase tryptophan fluorescence intensity upon ATP binding (*32*, *34*−*37*). It is reasonably assumed that this effect places the ASTs in the energy-transduction pathway of S1, a possibility that has stimulated and sustained interest in locating the residues responsible for the phenomena. Early efforts focused on tryptophans near to the active site (*7*) and on other tryptophans with side chains susceptible to chemical attack (*8*, *38*). We demonstrated Trp510's ATP sensitivity but did not rule out the possibility that other residues also contributed to the total fluorescence increase of S1 upon ATP binding (*12*, *13*). Recently, site-directed mutagenesis clarified the issue for two myosins. A mutant of Dictyostelium S1 replacing Trp510 with a tyrosine showed no tryptophan fluorescence change upon ATP binding (*10*). Mutants of smooth muscle myosin containing one tryptophan residue (Trp440, Trp510, or Trp595) were constructed and tested for a tryptophan fluorescence sensitivity to ATP binding to the active site (*11*). Only the mutant containing Trp510 sensed ATP binding. These data convincingly demonstrate that for practical purposes Trp510 is the only ATP-sensitive tryptophan in smooth and Dictyostelium S1. We provide here spectroscopic data supporting a similar conclusion for rabbit skeletal S1.

We spectroscopically isolate emission from selected tryptophan residues in S1. Werber et al. chemically reacted the indole side chain of Trp131 and showed that the modification minimally perturbs S1 structure (*6*). The reacted indole does not fluoresce, thereby eliminating Trp131 fluorescence from the modified protein signal. The difference of tryptophan fluorescence between native and modified S1 isolates native Trp131 emission. Fluorescence intensity and quenching constants of Trp131 (Table 1) do not distinguish among the nucleotides or trapped analogues, suggesting that the vicinity of Trp131 does not change conformation during the ATPase cycle and eliminating Trpl31 as an AST. Previously, we did a similar experiment on Trp510. Isolated native Trp510 fluorescence is ATP-sensitive (*12*, *13*), and experiments described here show that the Trp510 signal accounts for practically all of the fluorescence enhancement observed for skeletal S1 (Figure 1). We conclude that Trp510 is essentially the sole AST in skeletal S1.

Identification of Trp510 as the sole AST suggests a simple method, again based on difference spectroscopy, to characterize S1 structure local to this residue in the energy-transduction pathway. The difference of tryptophan fluorescence intensities between S1 and S1 + N, where N is bound nucleotide or trapped nucleotide analogue, produces the fluorescence emitted exclusively from Trp510. We observed Trp510 fluorescence enhancement and its quenching with both neutral (acrylamide) and anionic (I^-) quenchers. Acrylamide dynamically quenches Trp510 fluorescence, but the residue is inaccessible to I^- (Figure 2). We also confirmed our earlier observation that fluorescence intensity and acrylamide accessibility to Trp510 changes incrementally as S1 steps through the transient ATPase intermediates M → M* → M** → M^ defined in Scheme 1 (*12*, *13*). In contrast, an early tryptophan classification scheme for skeletal S1 identified three categories of tryptophans with long, intermediate, and short lifetimes (*2*). There, the AST lifetime was determined to be intermediate in duration and unaffected by acrylamide. Other work using photochemical modification showed the AST to be accessible to neutral charge chemicals such as 2,2,2-trichloroethanol (*8*), supporting the present findings. We cannot explain this discrepancy of findings but suggest that the AST lifetime would be isolated better from the difference lifetime decay curve obtained by subtracting the lifetime decay of S1 from S1 + N. Remember that such a difference decay curve would contain fluorescence from Trp510 in two inequivalent environments.

A New Technique for Quantifying Concentrations of Myosin ATPase Intermediates. Scheme 1 approximates the S1 ATPase cycle with three transient S1 structures induced by the ATP substrate undergoing hydrolysis. Trp510 undergoes fluorescence enhancement and change in its accessibility to acrylamide quenching due to the presence of ATP and other substrates that mimic the transient substrate in the ATPase cycle. We observe these quantities by isolating Trp510 emission with chemical or structural perturbants. The specific enhancements and quenching constants relate linearly to the fractional concentrations of the transient S1 conformations during ATPase, permitting their determination by least squares. We exploited this method to determine the fractional concentrations of the transient S1 conformations during ATPase. Our results agree with past findings in comparable conditions. This new technique for estimating the fractional concentrations of intermediates does not require time-resolved observations. The method could be useful for assaying the impact on S1 functionality of a disease-causing mutation or the specific chemical modification of a residue.

Table 4: Charged and Internal Quencher Amino Acid Residues within 10 Å from C_α of Five Tryptophans[a]

residues	Trp113	Trp131	Trp440	*Trp510*	Trp595
negative	Glu108		Glu435	*Glu499*	*Glu476*
				Glu501	Glu537
				Glu502	Glu539
				Glu509	Glu597
				Glu511	Asp547
positive	*Arg109*	Lys130	Arg444	Lys504	*Lys598*
	Arg 18		Lys436	Lys709	Lys600
	Lys107				Lys551
	Lys130				
internal quencher	Met114		Met437		Cys540
			Met441		

[a] Residues in italics are highly conserved from 82 different myosins. Trp440 and Trp595 are highly conserved only in the myosin II class (*40*).

Using the Crystal Structure of S1 To Help Find a Mechanism for AST Fluorescence Enhancement. Consider the crystal structure of S1 around Trp510 and the other tryptophan residues to surmise a possible mechanism for the ATP-sensitive tryptophan enhancement. The crystal structure of methylated chicken S1 shows that Trp113, 131, 440, and 510 are exposed to solvent to varying degrees and that Trp595 is largely protected from solvent (*39*). Other crystal structures in the presence of nucleotide analogues in smooth muscle myosin and DcS1 show similar degrees of solvent exposure for the equivalent tryptophan residues. We list the charged amino acid residues and internal quencher residues such as cysteine and methionine within 10 Å of the tryptophan residues of S1 in Table 4. The highly conserved amino acid residues from 82 different myosins are italicized (*40*). Negatively charged residues cluster around Trp510 and Trp595 unlike the other tryptophans. The inability of I^- to quench Trp510 matches to the cluster of negatively charged residues surrounding Trp510.

The considerable fluorescence enhancement accompanying ATP binding to S1 was explained initially by complex formation between a tryptophan indole ring and the purine ring of ATP (*41*). Alternatively, Bivin et al. (*29*) proposed that a change in the proximity of an ionizable group relative to a tryptophan indole accompanies substrate binding to the active site of S1 and causes the fluorescence enhancement. The existing crystal structures of S1 show that ionizable groups surround Trp510 and that the neighborhood of Trp510 undergoes conformation change upon nucleotide binding (*42*, *43*). We believe this is compelling circumstantial evidence supporting the latter proposal.

A third possible mechanism for the fluorescence enhancement has a quenching sulfur atom in methionine or cysteine withdrawing from the vicinity of a tryptophan upon ATP binding to S1 (*44*, *45*). Table 4 indicates that Trp113, Trp440, and Trp595 all have sulfur atoms within 7−10 Å (the average distance from the S atom of Met or Cys to the nine atoms of an indole ring). However, if the myosin family has a common mechanism for ATP enhancement of tryptophan fluorescence, then the withdrawal of sulfur is unlikely to participate in that mechanism since the sulfur-containing residues in chicken skeletal S1 are substituted with non-quenching residues in smooth S1 (Met114Leu, Met437Leu, Met44111e, and Cys540Trp) and DcS1 (Met114Leu, Met437Leu, Met441Leu, and Cys540Val) (*40*).

The Structure Perturbation Method for Isolating AST Emission. Finally, consider our new method for isolating Trp510 emission in S1. It totally preserves the native characteristics of the signal because it originates only from native S1 but is unable to do so from a pure conformational state of the S1 since the signal isolated combines emission from S1 with and without nucleotide. Our related work isolating emission from Trp131 (described in this paper) or Trp510 (using 5′IAF at SH1 as described previously (*12*, *13*)) does so from pure states of the S1. The inability of the heterogeneous Trp510 signal to isolate pure conformational states is recognized formally in the recursive formulas of eqs 9 and 10 that relate two single tryptophan quantities without defining their absolute value. Nevertheless, the two methods are equivalent in their ability to estimate the fractional concentrations of the myosin transient conformations associated with the ATPase cycle of Scheme 1. We also find that the two methods provide equivalent Trp510 fluorescence enhancements and solvent accessibilities when S1 assumes these transient conformations (compare data from Tables 2 and 3).

CONCLUSION

Like smooth and Dictyostelium S1, the AST in rabbit skeletal S1 is Trp510. Characterizable physical properties of the Trp510 in S1, including its fluorescence intensity and accessibility to quencher, vary dramatically in response to substrate binding to the active site of S1. These properties, observed from S1 in the presence of ATP, ADP, and the various phosphate analogues mimicking the ATPase transient intermediates, provide a means to measure the fractional concentrations of the intermediates during steady-state ATPase. The mechanism responsible for the fluorescence enhancement upon nucleotide binding appears to be related to changes in the proximity of the ionizable groups surrounding Trp510 (*29*).

ACKNOWLEDGMENT

We thank Dr. K. Ajtai for helpful discussions and Ms. S. P. Garamszegi for technical assistance on the project.

REFERENCES

1. Maita, T., Yajima, E., Nagata, S., Miyanishi, T., Nakayama, S., and Matsuda, G. (1991) *J. Biochem. 110*, 75−87.
2. Torgerson, P. M. (1984) *Biochemistry 23*, 3002−3007.
3. Muhlrad, A. (1989) *Biochemistry 28*, 4002−4010.
4. Muhlrad, A., Kasprzak, A. A., Ue, K., Ajtai, K., and Burghardt, T. P. (1986) *Biochim. Biophys. Acta 869*, 128−140.
5. Botts, J., Thomason, J. F., and Morales, M. F. (1989) *Proc. Natl. Acad. Sci. U.S.A. 86*, 2204−2208.
6. Werber, M. M., Peyser, Y. M., and Muhlrad, A. (1987) *Biochemistry 26*, 2903−2909.
7. Okamoto, Y., and Yount, R. G. (1985) *Proc. Natl. Acad. Sci. U.S.A. 82*, 1575−1579.
8. Papp, S. J., and Highsmith, S. (1993) *Biochim. Biophys. Acta 1202*, 169−172.
9. Hiratsuka, T. (1992) *J. Biol. Chem. 267*, 14949−14954.
10. Batra, R., and Manstein, D. J. (1999) *Biol. Chem. 380*, 1017−1023.
11. Yengo, C. M., Chrin, L., Rovner, A. S., and Berger, C. L. (2000) *Biophys. J. 78*, 242A.
12. Park, S., Ajtai, K., and Burghardt, T. P. (1996) *Biochim. Biophys. Acta 1296*, *1*−*4*.
13. Park, S., Ajtai, K., and Burghardt, T. P. (*1997*) *Biochemistry 36*, 3368−3372.

14. Park, S., and Burghardt, T. P. (2000) *Biophys. J. 78*, 115A.
15. Burghardt, T. P., and Ajtai, K. (1996) *Biophys. Chem. 60*, 119−133.
16. Ajtai, K., and Burghardt, T. P. (1995) *Biochemistry 34*, 15943−15952.
17. Bagshaw, C. R., and Trentham, D. R. (1974) *Biochem. J. 141*, 331−349.
18. Phan, B. C., Cheung, P., Stafford, W. F., and Reisler, E. (1996) *Biophys. Chem. 59*, 341−349.
19. Rayment, I., Smith, C., and Yount, R. G. (1996) *Annu. Rev. Physiol. 58*, 671−702.
20. Mendelson, R. A., Schneider, D. K., and Stone, D. B. (1996) *J. Mol. Biol. 256*, 1−7.
21. Gulick, A. M., Bauer, C. B., Thoden, J. B., and Rayment, I. (1997) *Biochemistry 36*, 11619−11628.
22. Tonomura, Y., Appel, P., and Morales, M. F. (1966) *Biochemistry 5*, 515−521.
23. Weeds, A. G., and Taylor, R. S. (1975) *Nature 257*, 54−56.
24. Burghardt, T. P., Garamszegi, S. P., Park, S., and Ajtai, K. (1998) *Biochemistry 37*, 8035−8047.
25. Ajtai, K., and Burghardt, T. P. (1992) *Biochemistry 31*, 4275−4282.
26. Ajtai, K., Poto, L., and Burghardt, T. P. (1990) *Biochemistry 29*, 7733−7741.
27. Ajtai, K., Ilich, P. J. K., Ringler, A., Sedarous, S. S., Toft, D. J., and Burghardt, T. P. (1992) *Biochemistry 31*, 12431−12440.
28. Park, S., Ajtai, K., and Burghardt, T. P. (1999) *Biochim. Biophys. Acta 1430*, 127−140.
29. Bivin, D. B., Kubota, S., Pearlstein, R., and Morales, M. F. (1993) *Proc. Natl. Acad. Sci. U.S.A. 90*, 6791−6795.
30. Park, S., Ajtai, K., and Burghardt, T. P. (1996) *Biophys. Chem. 63*, 67−80.
31. Eftink, M. R., and Ghiron, C. A. (1981) *Anal. Biochem. 114*, 199−227.
32. Werber, M. M., Szent-Gyorgyi, A. G., and Fasman, G. D. (1972) *Biochemistry 11*, 2872−2883.
33. Onishi, H., Ohtsuka, E., Ikehara, M., and Tonomura, Y. (1973) *J. Biochem. 74*, 435−450.
34. Marston, S. B., and Taylor, E. W. (1980) *J. Mol. Biol. 139*, 573−600.
35. Kurzawa-Goertz, S. E., Perreault-Micale, C. L., Trybus, K. M., Szent-Gyorgyi, A. G., and Geeves, M. A. (1998) *Biochemistry 37*, 7517−7525.
36. Kurzawa, S. E., Manstein, D. J., and Geeves, M. A. (1997) *Biochemistry 36*, 317−323.
37. Cremo, C. R., and Geeves, M. A. (1998) *Biochemistry 37*, 1969−1978.
38. Johnson, W. C., Jr., Bivin, D. B., Ue, K., and Morales, M. F. (1991) *Proc. Natl. Acad. Sci. U.S.A. 88*, 9748−9750.
39. Rayment, I., Rypniewski, W. R., Schmidt-Base, K., Smith, R., Tomchick, D. R., Benning, M. M., Winkelmann, D. A., Wesenberg, G., and Holden, H. M. (1993) *Science 261*, 50−58.
40. Cope, M. J. TV., Whisstock, J., Rayment, I., and Kendrick-Jones, J. (1996) *Structure 4*, 969−987.
41. Yoshino, H., Morita, F., and Yagi, K. (1972) *J. Biochem. (Tokyo) 72*, 1227−1235.
42. Smith, C. A., and Rayment, I. (*1996*) *Biochemistry 35*, 5404−5417.
43. Dominguez, R., Freyzon, Y., Trybus, K. M., and Cohen, C. (1998) *Cell 94*, 559−571.
44. Yuan, T., Weljie, A. M., and Vogel, H. J. (1998) *Biochemistry 37*, 3187−3195.
45. Reshetnyak, Y. K., Andreev, O. A., Borejdo, J., and Burstein, E. A. (1999) *Biophys. J. 76*, A50.

BI000945T